

Received Date : 24-Apr-2016

Revised Date : 05-Jun-2016

Accepted Date : 12-Jun-2016

Article type : Research Article

Synthesis, Structure-Activity Relationship Studies and Biological Evaluation of Novel 2,5-Disubstituted Indole Derivatives as Anticancer Agents

Hongyu Hu^{a#}, Jun Wu^{a#}, Mingtao Ao^a, Huiru Wang^a, Tongtong Zhou^a, Yuhua Xue^a, Yingkun Qiu^a, Meijuan Fang^{a*}, Zhen Wu^{a*}

^a School of Pharmaceutical Sciences and the Key Laboratory for Chemical Biology of Fujian Province, Xiamen University, South Xiang-An Road, Xiamen, 361102, China.

[#] These authors contribute equally to this paper

* Corresponding authors. Tel.: +86-592-2189868; Fax: +86-592-2189868.

E-mail address: fangmj@xmu.edu.cn (Meijuan Fang); wuzhen@xmu.edu.cn (Zhen Wu)

Abstract

Three novel series of 2,5-disubstituted indole derivatives were synthesized and evaluated *in vitro* for their anti-proliferative activity against human cancer cells and HIV-1 inhibition activity used as a read-out of cellular activity. Most compounds were found to have potent anticancer activity. In

This article has been accepted for publication and undergone full peer review but has not been through the copyediting, typesetting, pagination and proofreading process which may lead to differences between this version and the Version of Record. Please cite this article as an 'Accepted Article', doi: 10.1111/cbdd.12808

This article is protected by copyright. All rights reserved.

particular, **2c** and **3b** which showed effectively to repress HIV-1 transcription had a pan anti-proliferative activity in cervical cancer cells (Hela), breast cancer cells (MCF-7), liver cancer cells (HepG2) and lung cancer cells (H460 and A549). While **3b** exhibited high sensitivity to A549 cells with the IC₅₀ value 0.48±0.15 μM, **2c** showed high selectivity toward HepG2 cells with the IC₅₀ value 13.21±0.30 μM. With respect to the cellular mechanism of action, HepG2 cells treated with **2c** and A549 cells treated with **3b** for 24 hours were studied by annexin V/PI staining and western blot analysis, and results revealed that **2c** and **3b** may induce cancer cells apoptosis through inhibiting the phosphorylation at Ser2 of RNAPII CTD which can be phosphorylated by cyclin-dependent kinase 9. These studies indicated that **2c** and **3b** may develop as potent lead compounds in the therapy of cancer. However, determining their roles in preventing HIV-1 still requires further intensive study.

Key words: 2,5-disubstituted indole derivatives; anticancer activity; HIV-1 inhibition activity; phosphorylation; RNA polymerase II

Indole ring system as one of the most ubiquitous heterocycles in nature has been becoming an important structural component in many pharmaceutical agents, such as antidepressant (1), anticonvulsant (2,3), antifungal (4), antiviral (5) and anti-inflammatory (6), particularly in discovery of new antitumor agents (7) or HIV inhibitors (3,8,9). In recent years, increasing numbers of researchers from both industry and academia have embarked on the development of new indole-based small molecules as potent antitumor agents (10) or HIV inhibitors (9). For example, small molecule Bcl-2 antagonist Obatoclax (phase III, Figure 1) could antagonize MCL-1 and overcome MCL-1-mediated resistance to apoptosis (11). In addition, Sunitinib (Figure 1), a multi-targeted receptor tyrosine kinase inhibitor containing indolin-2-one moiety, was approved by the FDA for the treatment of advanced renal cell carcinoma (RCC) and gastrointestinal stromal tumors (GISTs) (12). Moreover, benzyl-1*H*-indole derivatives also possessed prominent antitumor activity (13), such as a novel synthetic microtubule inhibitor D-24851 (Phase I/II, Figure 1) (14). On the other hand, 3-aryl-phospho-indole (API) was developed as novel HIV-1 non-nucleoside reverse transcriptase inhibitors (15,16). For example, API-18 (Figure 1) possessed excellent potency against wild-type HIV-1 with the

EC₅₀ value 0.1 nM (15,16). All these prompted us to investigate new potential anticancer agents and HIV inhibitors with the indole structure which had 2nd and 5th position substitutions.

Figure 1. Structures of four compounds bearing indole-based moiety

Messenger RNA (mRNA) is a large family of RNA molecules that convey genetic information from DNA to the ribosome, and inhibition of mRNA synthesis can reduce cancer cells apoptosis (17) which is an attractive strategy for cancer treatment (18). mRNA synthesis by RNA polymerase II (RNAPII) is regulated by the phosphorylation of RNAPII's C-terminal domain (CTD) in which Ser2 can be phosphorylated by cyclin-dependent kinase 9 (CDK9) (19). CDK9 was also found to be a component of the multiprotein complex TAK/P-TEFb, which is an elongation factor for RNAPII-directed transcription and functions by phosphorylating the CTD of the largest subunit of RNAPII (16). Since the discovery that the CDK inhibitor flavopiridol induces cell apoptosis by inhibiting CDK9 (20), the enzyme has been a target for anticancer drug design. There have been some other CDK9's inhibitors applied in cancer therapy, for example SCH727965 for breast cancer (21), AT7519 for refractory solid tumors (22) and SNS-032 for chronic lymphocytic leukemia (23). On the other hand, P-TEFb composed of Cdk9 and cyclin T1 is a required cellular cofactor for the human immunodeficiency virus (HIV-1) transactivator, Tat. As CDK9 is a key component of P-TEFb, CDK9 inhibitors DRB, seliciclib and flavopiridol have been reported to inhibit the HIV-1 virus transcription and replication effectively (24). Over all, CDK9 inhibitors can be effective drugs for cancers, HIV-1 and some other diseases.

In this work, we employed indole structural scaffold as a pharmaceutical core linker to design and synthesize three series of structurally related indole derivatives (Scheme 1). All synthesized compounds were subsequently evaluated *in vitro* for anti-proliferative activity against three human cancer cell lines (Hela, HepG2 and A549) and HIV-1 inhibition activity used as a read-out of cellular activity. Then, compounds **2c** and **3b** with good anti-proliferative activity against cancer cells and excellent HIV-1 inhibition activity were selected for further cellular mechanism studies which included testing the induction of cell apoptosis, and checking the level of cleaved PARP (the mark of apoptosis), the phosphorylation level at Ser2 of RNAPII CTD and the expression level of CDK9 (25).

Scheme 1. 2,5-Disubstituted indole derivatives

Experimental Section

Chemistry

All reagents were purchased and used without further purification, unless otherwise indicated.

Reactions were magnetically stirred and monitored by thin-layer chromatography (TLC) on Merck silica gel 60F-254 by fluorescence. All of the final compounds were purified by column chromatography. $^1\text{H-NMR}$ and $^{13}\text{C-NMR}$ spectra were obtained using a Bruker AV2 600 Ultra shield spectrometer at 600 and 150 MHz respectively, chemical shifts were given in parts per million (ppm) relative to tetramethylsilane (TMS) as an internal standard. Multiplicities were abbreviated as follows: single (s), doublet (d), doublet-doublet (dd), doublet-triplet (dt), triplet (t), triplet-triplet (tt), triplet-doublet (td), quartet (q), quartet-doublet (qd), multiplet (m), and broad signal (brs). High-resolution mass spectral (HRMS) data were acquired on a Q Exactive. Melting points were measured on a SGW X-4 micro-melting point spectrometer and were uncorrected.

***N*-*o*-tolylcycloadamantanecarboxamide (5)**

A mixture of *o*-toluidine (10.0 mmol, 1.07 g), 1-adamantanecarbonyl chloride (10.0 mmol, 1.98 g) and anhydrous potassium carbonate (7.0 mmol, 0.97 g) in toluene (50 mL) was stirred at room temperature for 4 hours. The resulting solid was filtered off and then stirred at room temperature for 1.5 h with 50 mL of H_2O . The solid was filtered off and recrystallized from EtOH. White solid (75.5%). $^1\text{H-NMR}$ (600 MHz, CDCl_3): δ 7.88 (d, $J = 8.07$ Hz, 1H), 7.18-7.24 (m, 2H), 7.17 (d, $J = 7.52$ Hz, 1H), 7.05 (dt, $J = 1.10, 7.43$ Hz, 1H), 2.26 (s, 3H), 2.11 (brs, 3H), 1.99 (d, $J = 2.57$ Hz, 6H), 1.77 (q, $J = 12.29$ Hz, 6H). ESI-HRMS (+): m/z calcd for $\text{C}_{18}\text{H}_{24}\text{NO}^+$ $[\text{M}+\text{H}]^+$ 270.1852, found 270.1853; calcd for $\text{C}_{18}\text{H}_{23}\text{NONa}^+$ $[\text{M}+\text{Na}]^+$ 292.1672, found 292.1669.

2-Adamantane-1*H*-indole (6)

A stirred solution of amide **5** (10.0 mmol, 2.69 g) in THF (50 mL) under a N₂ atmosphere was maintained at an internal temperature of -5 to 5°C and treated dropwise with 0.1-0.15 mol of *n*-BuLi as 2.5 M *n*-BuLi in hexane. The stirred mixture was kept at ambient temperature, cooled in an ice bath, and treated dropwise with 2 M HCl (12 mL). The organic layer was separated and the aqueous layer washed with C₆H₆. The combined organic layer was dried with anhydrous MgSO₄, filtered, and concentrated. The residue was purified by column chromatography to get white solid with the yield of 83%. ¹H-NMR (600 MHz, CDCl₃): δ 7.30 (d, *J* = 7.89 Hz, 1H), 7.18 (dd, *J* = 0.55, 8.07 Hz, 1H), 6.88 (dt, *J* = 1.10, 7.52 Hz, 1H), 6.77-6.83 (m, 1H), 5.98 (d, *J* = 0.55 Hz, 1H), 1.97 (d, *J* = 2.57 Hz, 3H), 1.93 (d, *J* = 2.93 Hz, 6H), 1.73 (brs, 6H). ESI-HRMS (+): *m/z* calcd for C₁₈H₂₂N⁺ [M+H]⁺ 252.1747, found 252.1748; calcd for C₁₈H₂₁NNa⁺ [M+Na]⁺ 274.1566, found 274.1568.

2-Adamantane-5-nitro-1*H*-indole (7)

In a 250 mL round-bottom flask, 2-adamantane-1*H*-indole (10 mmol, 2.51 g) was dissolved in H₂SO₄ (10 mL) after vigorous stirring. In a separate flask, NaNO₃ (11 mmol, 0.94 g) was dissolved in H₂SO₄ (10 mL), also after vigorous stirring, and added dropwise *via* addition funnel to the 2-adamantane-1*H*-indole. After addition, the reaction was stirred for another 10 min and then poured into ice water (200 mL), precipitating a yellow product. The product was isolated via filtration and washed with cold water. After 12 h of drying under vacuum, 2.89 g of yellow product was isolated (97%). ¹H-NMR (600 MHz, DMSO-*d*₆): δ 11.65 (brs, 1H), 8.44 (d, *J* = 2.20 Hz, 1H), 7.93 (dd, *J* = 2.20, 8.99 Hz, 1H), 7.44 (d, *J* = 8.80 Hz, 1H), 6.38 (d, *J* = 1.47 Hz, 1H), 2.07 (brs, 3H), 1.98 (brs, 6H), 1.67-1.81 (m, 6H). ¹³C-NMR (150 MHz, DMSO-*d*₆): δ 154.0, 140.8, 139.9, 127.7, 116.9, 116.3, 111.4, 98.2, 41.9, 36.6, 34.1, 28.2. ESI-HRMS (+): *m/z* calcd for C₁₈H₂₁N₂O₂⁺ [M+H]⁺ 297.1598, found 297.1599; calcd for C₁₈H₂₀N₂O₂Na⁺ [M+Na]⁺ 319.1417, found 319.1417.

2-Adamantane-1*H*-indol-5-amine (**8**)

Compound **7** (10 mmol, 2.96 g) was dissolved in ethanol (150 mL), 10% Pd/C was added (300 mg), and the mixture was subjected to H₂ (38 psi) using a Parr hydrogenator for 3.5 h. The mixture was filtered over Celite, which was washed with methanol. After concentration and drying under vacuum, 2.5 g of a brown powder (94%) was isolated. ¹H-NMR (600 MHz, CDCl₃): δ 7.80 (brs, 1H), 7.10 (d, *J* = 8.44 Hz, 1H), 6.86 (d, *J* = 2.20 Hz, 1H), 6.57 (dd, *J* = 2.20, 8.44 Hz, 1H), 6.05 (dd, *J* = 0.73, 2.20 Hz, 1H), 3.23-3.65 (m, 2H), 2.09 (brs, 3H), 1.96 (d, *J* = 2.38 Hz, 6H), 1.78 (q, *J* = 12.17 Hz, 6H). ¹³C-NMR (150 MHz, CDCl₃): δ 149.9, 139.3, 130.3, 129.4, 111.6, 110.8, 105.3, 95.5, 42.6, 36.8, 33.7, 28.5. ESI-HRMS (+): *m/z* calcd for C₁₈H₂₃N₂⁺ [M+H]⁺ 267.1856, found 267.1858.

N-(2-adamantane-1*H*-indol-5-yl)-benzamide (**1a**)

A mixture of 2-adamantane-1*H*-indol-5-amine **8** (10.0 mmol, 2.66 g), benzoyl chloride (10.0 mmol, 1.41 g) and anhydrous potassium carbonate (7.0 mmol, 0.97 g) in toluene (50 mL) was stirred at room temperature for 4 h. The resulting solids was filtered off and then stirred at room temperature for 1.5 h with 50 mL of H₂O. The solid was filtered off and recrystallized from EtOH. White solid (78.7%). Mp: 263-265°C ¹H-NMR (600 MHz, DMSO-*d*₆): δ 10.82 (s, 1H), 10.04 (s, 1H), 7.98 (d, *J* = 7.34 Hz, 2H), 7.86 (d, *J* = 0.92 Hz, 1H), 7.55-7.59 (m, 1H), 7.50-7.54 (m, 2H), 7.32 (dd, *J* = 1.74, 8.53 Hz, 1H), 7.25 (d, *J* = 8.62 Hz, 1H), 6.07 (d, *J* = 1.65 Hz, 1H), 2.07 (brs, 3H), 1.98 (d, *J* = 2.20 Hz, 6H), 1.73-1.81 (m, 6H). ¹³C-NMR (150 MHz, DMSO-*d*₆): δ 165.4, 150.8, 135.9, 133.5, 131.6, 131.1, 128.7, 128.0, 128.0, 115.6, 112.3, 110.8, 95.6, 42.3, 36.8, 33.9, 28.4. ESI-HRMS (+): *m/z* calcd for C₂₅H₂₇N₂O⁺ [M+H]⁺ 371.2118, found 371.2111; calcd for C₂₅H₂₆N₂ONa⁺ [M+Na]⁺ 393.1937, found 393.1929.

At the Series A, the other target compounds were synthesized following the general procedure as described above with the yield of 84–89%. Their structures were also confirmed (see 'Supporting Information').

5-Isocyanato-1*H*-indole-adamantane (9)

A solution of 2-adamantane-1*H*-indol-5-amine **8** (10.0 mmol, 2.66 g) dissolved in THF (80 mL) was slowly dropped into a stirred solution of triphosgene (10.0 mmol, 2.98 g) in THF (10 mL) by using a constant-pressure dropping funnel. NEt₃ (21.0 mmol, 3 mL) was then added slowly to the reaction mixture after **8** were added. The reaction mixture was stirred at 0 °C for 2 h. After completion of the reaction, the mixture was concentrated and purified by column chromatography using appropriate mixtures of EtOAc and PE to yield the titled compound. White solid (61.5%). ¹H NMR (600 MHz, CDCl₃): δ 8.01 (brs, 1H), 7.21 (d, *J* = 8.44 Hz, 1H), 6.85 (dd, *J* = 2.02, 8.44 Hz, 1H), 6.17 (d, *J* = 1.47 Hz, 1H), 2.07-2.15 (m, 3H), 1.98 (brs, 6H), 1.74-1.85 (m, 6H). ¹³C-NMR (150 MHz, CDCl₃): δ 151.0, 133.2, 129.0, 125.1, 123.6, 118.1, 115.5, 111.1, 96.4, 42.5, 36.7, 33.8, 28.4.

1-(4-Chloro-2-methoxyphenyl)-3-(1*H*-indol-2-adamantine-5-yl)urea (2c)

A mixture of 5-isocyanato-1*H*-indole-adamantine **9** (0.4 mmol, 0.12 g) in toluene (5 mL) and 4-chloro-2-methoxybenzenamine (0.4 mmol) was heated at 60 °C for 4 h. After completion of the reaction, the mixture was concentrated and purified by column chromatography using appropriate mixtures of CH₂Cl₂ and MeOH to get the titled compound. White solid (84.2%). Mp: 253-255 °C. ¹H-NMR (600 MHz, DMSO-*d*₆): δ 10.73 (s, 1H), 8.69 (s, 1H), 8.38 (s, 1H), 7.56 (d, *J* = 1.28 Hz, 1H), 7.45 (d, *J* = 2.02 Hz, 1H), 7.27 (d, *J* = 8.62 Hz, 1H), 7.21 (d, *J* = 8.62 Hz, 1H), 7.00 (dd, *J* = 1.83, 8.44 Hz, 1H), 6.94 (dd, *J* = 2.11, 8.53 Hz, 1H), 6.03 (d, *J* = 1.47 Hz, 1H), 3.83 (s, 3H), 2.05 (brs, 3H), 1.96 (brs, 6H), 1.70-1.80 (m, 6H). ¹³C-NMR (150 MHz, DMSO-*d*₆): δ 155.0, 153.4, 150.7, 141.0, 132.9, 131.2, 130.1, 128.4, 114.3, 113.4, 111.1, 110.4, 103.1, 95.4, 56.2, 42.3, 36.8, 33.9, 28.4. ESI-HRMS (+): *m/z* calcd for C₂₆H₂₉ClN₃O₂⁺ [M+H]⁺ 450.1943, found 450.1942; calcd for C₂₆H₂₈ClN₃O₂Na⁺ [M+Na]⁺ 472.1762, found 472.1760.

At the Series B, the other target compounds were synthesized following the general procedure as described above with the yield of 81–89%. Their structures were also confirmed (see ‘Supporting Information’).

(E)-ethyl 2-(2-(4-nitrophenyl)hydrazono)propanoate (11)

A solution of 1-(4-nitrophenyl) hydrazine (65 mmol, 10.0 g) in EtOH (100 mL) was treated with ethyl 2-oxopropanoate (72 mmol, 8.4 g), The mixture has been stirred at 78°C for 2 h, when TLC indicated that the reaction had gone to completion. On cooling, Precipitated complex was filtered, washed with EtOH, and dried to afford (E)-ethyl 2-(2-(4-nitrophenyl)hydrazono)propanoate (**11**) as a yellow solid. Yield: 14.5 g (88.9%). ¹H-NMR (600 MHz, CDCl₃): δ 8.21 (d, *J* = 8.99 Hz, 2H), 8.09 (s, 1H), 7.28 (d, *J* = 8.99 Hz, 2H), 4.32-4.39 (m, 2H), 2.17 (s, 3H), 1.40 (t, *J* = 7.06 Hz, 3H).

Ethyl 5-nitro-1H-indole-2-carboxylate (12)

The solution of (E)-ethyl 2-(2-(4-nitrophenyl)hydrazono)propanoate **11** (42 mmol, 10 g) in polyphosphoric acids was stirred at 100°C for 2 h, and monitored by TLC analysis. After completion of the reaction, the mixture was diluted with a lot of water. Precipitated complex was filtered, washed with water, and dried to afford ethyl 5-nitro-1H-indole-2-carboxylate (**12**) as a green solid. Yield: 8.1 g (82.4%). ¹H-NMR (600 MHz, DMSO-d₆): δ 12.58 (brs, 1H), 8.71 (d, *J* = 2.02 Hz, 1H), 8.12 (dd, *J* = 2.20, 9.17 Hz, 1H), 7.61 (d, *J* = 9.17 Hz, 1H), 7.42 (d, *J* = 0.92 Hz, 1H), 4.37 (q, *J* = 7.09 Hz, 2H), 1.35 (t, *J* = 7.15 Hz, 3H).

Ethyl 5-amino-1H-indole-2-carboxylate (13)

Compound **12** (10 mmol, 2.34 g) was dissolved in ethanol (150 mL), 10% Pd/C was added (300 mg), and the mixture was subjected to H₂ (38 psi) using a Parr hydrogenator for 3.5 h. The mixture was filtered over Celite, which was washed with methanol. After concentration and drying under vacuum, 1.86 g of a brown powder (91.2%) was isolated. ¹H-NMR (600 MHz, DMSO-d₆): δ 11.38 (brs, 1H), 7.16-7.19 (m, 1H), 6.84 (dd, *J* = 0.83, 2.11 Hz, 1H), 6.69-6.73 (m, 2H), 4.63 (brs, 2H), 4.29 (q, *J* = 7.09 Hz, 2H), 1.31 (t, *J* = 7.15 Hz, 3H). ¹³C-NMR (150 MHz, DMSO-d₆): δ 161.9, 142.5, 132.0, 128.2, 127.1, 117.2, 113.2, 106.6, 103.6, 60.6, 14.8.

Ethyl 5-benzamido-1*H*-indole-2-carboxylate (**14**)

A mixture of ethyl 5-amino-1*H*-indole-2-carboxylate **13** (10.0 mmol, 2.04 g), benzoyl chloride (10.0 mmol, 1.41 g) and anhydrous potassium carbonate (7.0 mmol, 0.97 g) in toluene (50 mL) was stirred at room temperature for 4 h. The resulting solid was filtered off and then stirred at room temperature for 1.5 h with 50 mL of H₂O. The solid was filtered off and recrystallized from EtOH. White solid (75.5%). ¹H-NMR (600 MHz, DMSO-*d*₆): δ 11.87 (brs, 1H), 10.23 (brs, 1H), 8.16 (s, 1H), 7.99 (d, *J* = 7.34 Hz, 2H), 7.56-7.61 (m, 2H), 7.50-7.55 (m, 2H), 7.43 (d, *J* = 8.80 Hz, 1H), 7.15 (s, 1H), 4.35 (q, *J* = 7.09 Hz, 2H), 1.35 (t, *J* = 7.15 Hz, 3H); ¹³C-NMR (150 MHz, DMSO-*d*₆): δ 165.7, 161.7, 135.7, 135.0, 132.6, 131.8, 128.8, 128.3, 128.1, 127.0, 120.6, 113.7, 112.9, 108.2, 60.9, 14.8; ESI-HRMS (+): *m/z* calcd for C₁₈H₁₇N₂O₃⁺ [M+H]⁺ 309.1234, found 309.1225; calcd for C₁₈H₁₆N₂O₃Na⁺ [M+Na]⁺ 331.1053, found 331.1053.

5-Benzamido-1*H*-indole-2-carbohydrazide (**15**)

To a solution of ethyl 5-benzamido-1*H*-indole-2-carboxylate (5 mmol, 1.54 g) in 95% ethyl alcohol (10 mL) hydrazine hydrate (10 mL) was added, and the reaction mixture was heated under reflux for 8 h. The hydrazide was obtained in quantitative yields directly after evaporation of the reaction solution without any additional purification step. White solid (85.5%). ¹H-NMR (600 MHz, DMSO-*d*₆): δ 11.58 (s, 1H), 10.14 (s, 1H), 9.76 (brs, 1H), 8.07 (s, 1H), 7.97 (d, *J* = 7.15 Hz, 2H), 7.56-7.60 (m, 1H), 7.51-7.55 (m, 2H), 7.47 (dd, *J* = 1.65, 8.80 Hz, 1H), 7.39 (d, *J* = 8.80 Hz, 1H), 7.07 (d, *J* = 1.47 Hz, 1H), 4.50 (s, 2H). ¹³C-NMR (150 MHz, DMSO-*d*₆): δ 165.6, 161.6, 135.8, 133.9, 132.2, 131.7, 131.6, 128.8, 128.0, 127.3, 118.9, 113.3, 112.5, 102.4. ESI-HRMS (+): *m/z* calcd for C₁₆H₁₅N₄O₂⁺ [M+H]⁺ 295.119, found 295.1182; calcd for C₁₆H₁₄N₄O₂Na⁺ [M+Na]⁺ 317.1009, found 317.1004.

(*E*)-*N'*-(4-Methylbenzylidene)-5-benzamido-1*H*-indole-2-carbohydrazide (**3b**)

To a solution of 5-benzamido-1*H*-indole-2-carbohydrazide **15** (0.25 mmol, 0.075 g) in ethanol (5 mL), 4-methylbenzaldehyde (0.3 mmol, 0.036 g) was added, and the reaction mixture was heated at reflux for 8 h, and monitored by TLC analysis. After completion of the reaction, the mixture was

This article is protected by copyright. All rights reserved.

concentrated. Then the residue was purified by column chromatography to get white solid with the yield of 83.6%. Mp: 297-298°C. ¹H-NMR (600 MHz, DMSO-d₆): δ 11.83 (brs, 1H), 11.79 (brs, 1H), 10.18 (s, 1H), 8.44 (brs, 1H), 8.18 (brs, 1H), 8.00 (d, *J* = 7.15 Hz, 2H), 7.66 (d, *J* = 7.52 Hz, 2H), 7.57-7.61 (m, 1H), 7.51-7.56 (m, 3H), 7.45 (d, *J* = 8.62 Hz, 1H), 7.30 (d, *J* = 7.89 Hz, 3H), 2.36 (s, 3H). ¹³C-NMR (150 MHz, DMSO-d₆): δ 165.7, 158.0, 147.7, 140.3, 135.7, 134.5, 132.5, 132.1, 131.8, 131.2, 129.9, 128.8, 128.0, 127.5, 127.3, 119.8, 113.5, 112.7, 104.1, 21.5. ESI-HRMS (+): *m/z* calcd for C₂₄H₂₁N₄O₂⁺ [M+H]⁺ 397.1659, found 397.1651; calcd for C₂₄H₂₀N₄O₂Na⁺ [M+Na]⁺ 419.1478, found 419.1470.

At the Series C, the other target compounds were synthesized following the general procedure as described above with the yield of 84–90%. Their structures were also confirmed (see ‘Supporting Information’).

Biological assays

Luciferase assay

Inhibition of HIV-1 transcription was measured in NH2 cell line using luciferase assay. NH2 was a stable cell line based on HeLa cells with an integrated HIV-1 LTR-luciferase reporter gene and stably expressing PCDNA3-Tat-flag, the expression level of report gene luciferase could reveal the HIV-1 transcription level. In this experiment, NH2 cells in 48-well plate were treated with compounds (0.2 μM, 2 μM and 20 μM) for 8 hours and 0.2 μM flavopiridol as the positive control respectively, after treatment cell lysates were normalized and measured luciferase activity using luciferase kit from Promega.

MTT toxicity assay

All the cancer cells used in MTT assay were cultured in DMEM medium (Life Technological) with 10% FBS. The MTT reagent 3-(4,5-Dimethyl-2-thiazolyl)-2,5-diphenyl-2H-tetrazolium bromide was purchased from sigma (M2128). Cells were cultured in 96-well plate with 100 μL medium and the

total amount of cells in each well was about 1×10^4 . Concentration gradients (5-7 different concentrations) of each compound were then added to cells (six repeats), cisplatin (DDP) as the positive control and dimethyl sulfoxide (DMSO) as the negative control. After 48 hours treatment, 10 μ L MTT (5 mg/mL) was added to each wells staining for 4 hours in cell incubator. Then in each well, medium was discarded and 100 μ L DMSO was used, after short time shaking, the light intensity was measured at a wavelength of 490 nm. At last, the IC_{50} values (concentrations required to inhibit 50% of cell growth) were calculated using GraphPad Prism 5 software.

Annexin V/PI staining and cell cycle analysis

Cells were cultured in six-well with about 1×10^5 cells in each well and treated with varying concentrations of **2c** or **3b** for 24 hours respectively. Then the cell apoptosis analysis was performed following the protocols (BD Bioscience). After stained with FITC annexin V/PI, the apoptosis status was analyzed using a Beckman Epics Altra Culter and data were analyzed with EXP032 software. The status and percentage of cells undergoing apoptosis were defined as early apoptosis (annexin V-positive and PI-negative) and late apoptosis (annexin V-positive and PI-positive).

Western blot analysis

To check the proteins changes after compounds treatment, the western blot analysis was performed. After 24 hours treatment with varying concentrations of **2c** and **3b**, cells on plate were washed with $1 \times$ PBS and added with $1 \times$ SDS loading buffer for lysing. The samples were boiled (100°C 10 min) and used for western blot analysis. The phosphorylation level of CTD ser2 (p-Ser2, A300-654A, Bethyl), total CDK9 (11705-1-AP, proteintech) protein level and cleaved PARP (9542, CST) were tested, and α -Tubulin (T-6074, sigma) was used as a control. Both anti-rabbit and anti-mouse IgG were purchased from sigma.

Result and Discussion

Chemistry

In this work, we synthesized three series of novel chemically modified indole compounds including an adamantane group or a *N*'-(substituted methylene)-carbohydrazide group at the 2nd position and a substituted urea group or a substituted benzamide group at the 5th position in the indole system.

First, we synthesized 2-adamantane-1*H*-indol-5-amine (**8**). The general chemistry for the synthesis of **8** was adapted from the methods reported previously (26-28) and outlined in Scheme 2. Briefly, treatment of 1-adamantanecarboxylic acid chloride (**4**) with *o*-toluidine resulted in *N*-*o*-tolylcycloadamantanecarboxamide (**5**), followed by dropwise add of 1.4 or 1.6 M *n*-Butyllithium in hexane to get the corresponding 2-adamantane-1*H*-indole (**6**). **8** can be easily formed through nitration and catalytic hydrogenation of compound **6**. **8** was converted to Series **A** (**1a-1e**, Scheme 3) by reaction with benzoyl chloride and 5-isocyanato-1*H*-indole-adamantane (**9**) was obtained by reaction with **8** and triphosgene. **9** converted to Series **B** (**2a-2p**, Scheme 3) by reaction with corresponding amine (29).

Scheme 2. Synthesis of 2-(adamantan-1-yl)-1*H*-indol-5-amine. Reagents and conditions: (a) toluene, *o*-toluidine, K₂CO₃, r.t., 4 h; (b) *n*-BuLi, THF, 0°C, N₂, 3 h; (c) NH₄NO₃, H₂SO₄, 0°C, 1 h; (d) Fe, AcOH, H₂O, EtOH, 70°C, 2 h.

Scheme 3. Synthesis of series **A** and series **B**. Reagents and conditions: (a) benzoyl chloride, toluene, 60°C, 8 h; (b) triphosgene, THF, trimethylamine, 0°C, 4 h; (c) R-NH₂, toluene, 60°C, 4 h.

We synthesized ethyl 5-amino-1*H*-indole-2-carboxylate (**13**). The general chemistry for the synthesis of **13** was adapted from the methods reported previously (28) and outlined in Scheme 4. **13** was acylated to get the ethyl 5-benzamido-1*H*-indole-2-carboxylate (**14**) by reacting with benzoyl chloride in toluene at 60°C for 4 h. 5-Benzamido-1*H*-indole-2-carbohydrazid (**15**) were obtained by dropping hydrazine hydrate in **14** ethanol (30). The desired analogs (**3a-3s**, Scheme 4) were obtained by dropwise addition of corresponding aldehyde in **15** ethanol solution.

Scheme 4. Synthesis of series **C**. Reagents and conditions: (a) ethyl 2-oxopropanoate, EtOH, reflux, 2 h; (b) polyphosphoric acid, 100°C, 1 h; (c) Fe, AcOH, H₂O, EtOH, 70°C, 2 h. (d) benzoyl chloride, toluene, 60°C, 8 h; (e) Hydrazine hydrate, EtOH, reflux, 6 h; (f) RCHO, EtOH, reflux, 8 h.

Anti-proliferative activity in human cancer cell lines based on MTT assay and structure-activity relationship

All synthesized compounds were first evaluated the anti-proliferative activity against Hela cancer cells. Their anti-proliferative activity was summarized in table 1. The result indicated that most compounds showed a moderate anti-proliferative activity against Hela cells such as **2c** with the IC₅₀ value 15.54 μM and **3b** with the IC₅₀ value 8.70 μM.

Considering the whole result in Hela cells, attempts were made to establish the structure-activity relationship (SAR) among the tested compounds. Firstly, we found that in the 2-adamantane-5-substituted benzamide-indole series (series **A**), all compounds had good anti-proliferative activity against Hela cells. Substitutions at phenyl ring had little effect on compound's anti-proliferative activity, and replacement of phenyl ring with pyridyl ring showed similar cellular anti-proliferative activity (**Table 1, 1d vs 1e**). Among the 2-adamantane-5-substituted urea-indole derivatives (series **B**), aryl substituted compounds (**2a~2g** and **2n~2p**) were generally more active against Hela cells than alkylated derivatives (**2h~2m**). Among aryl substituted compounds, substitution at C4-phenyl ring played an important role in enhancing cellular anti-proliferative activity, but substitution at C3-phenyl ring was unhelpful for anti-proliferative activity (**Table 1, 2a~2d vs 2e~2g**). In addition, compared with compound **2d** with hydrophobic group (CH₃) at *o*- position of phenyl ring, compound **2c** bearing *o*- hydrogen bond acceptor function group (OCH₃) exhibited weak anti-proliferative activity. In the 2-[*N'*-(substituted methylene)-carbohydrazide]-5-benzamide-indole derivatives (series **C**), different substituted groups and positions of the phenyl ring introduced at the *N'*-methylene position displayed an important relationship with anti-proliferative activity. Compared with compound **3a** (phenyl, IC₅₀>100 μM), compounds **3b**, **3c** and **3d** which had methyl (CH₃), carboxyl (COOH) and ylthiomethyl (SCH₃) group at the C-4 position of phenyl ring respectively enhanced cellular anti-proliferative activity with an over 10-fold gain in cellular toxicity, suggesting that the

Accepted Article

impact of the substituent at the C-4 position of the phenyl ring was significant. However, compound **3g** with the 4-OCH₃ substitution at phenyl ring was no active with IC₅₀ value up to 100 μM. To further evaluate the importance of substituted position at the phenyl ring, compounds **3h** (2-OCH₃), **3i** (3,5-OCH₃), **3j** (3,4-OCH₃), **3k** (2,3-OCH₃) and **3l** (2,3,4-OCH₃) were subsequently synthesized. Biological evaluation revealed that two methoxy groups were introduced at *m*- position (**3i**, IC₅₀, 1.67 μM) to be a determining factor for anti-proliferative activities against Hela cells. Additionally, compounds **3q** (IC₅₀, 24.7 μM) and **3r** (IC₅₀, 73.5 μM) both possessing a bicyclic aromatic ring system at the *N'*-methylene position showed increased activities against Hela cells compared with the compounds **3o** (IC₅₀, over 100 μM) and **3h** (IC₅₀, over 100 μM) both bearing a single aromatic cyclic ring system at the *N'*-methylene position, respectively. The IC₅₀ value of compound **3s** was over 100 μM, indicating that the introduction of *n*-alkyl group to the pharmaceutical core may be unfavorable for anti-proliferative properties, together with the results based upon **B** series.

Furthermore, all compounds with IC₅₀ value below 20 μM were evaluated for their *in vitro* anti-proliferation activities against another two cancer cell lines, which were HepG2 and A549, with the positive contrast drug DDP. As shown in Table 1, the results indicated that most of the target compounds could also effectively inhibit the proliferation of HepG2 and A549 cells. Interestingly, compound **2d** with adamantane substitution at the 2nd position of indole ring and (4-chloro-2-methyl) phenyl substitution at urea end showed minimum IC₅₀ value (0.80 μM) with highest inhibition among the compounds in the series against HepG2 cells. Against A549 cells, compound **3d** showed the highest inhibition with IC₅₀ value of 0.16 μM, compounds **2a** (IC₅₀, 0.50 μM) and **3b** (IC₅₀, 0.48 μM) showed more inhibition than the standard drug DDP (IC₅₀, 1.83 μM).

Table 1. Anti-proliferative activity (IC₅₀, μM) against cancer cells of 2,5-disubstituted indole derivatives

HIV-1 inhibition activity

It is reported that phosphorylation of the RNA polymerase II carboxyl-terminal domain (RNAPII CTD) by CDK9 is directly responsible for human immunodeficiency virus type 1 tat-activated transcriptional elongation (31). So the HIV activity may be used as a read-out of cellular activity. After evaluating compounds' anti-proliferative activity against cancer cells by MTT assay, we then used luciferase assay to test whether these compounds can inhibit HIV-1 transcription. Interestingly, 20 kinds among all tested compounds had the HIV-1 inhibition activity as shown in table 2, besides **2c** and **3b** were more potential than others. These compounds bearing both anticancer activity and anti-HIV activity may have dual utility.

Table 2. HIV-1 inhibition activity

Cellular mechanism of action

According to the MTT assay and HIV-1 inhibition assay, compounds **2c** and **3b** were selected for further cellular mechanism studies. Firstly, a range of human cancer cell lines were treated with these two compounds for 48 hours, including breast cancer cells (MCF-7), liver cancer cells (HepG2) and lung cancer cells (H460 and A549). The MTT assay's results showed that **2c** and **3b** had a pan anti-proliferative activity in these cancer cell lines, but A549 cells were relative sensitive to **3b** with the IC₅₀ value 0.48 μM and HepG2 cells to **2c** with the IC₅₀ value 13.21 μM as shown in Table 3. Next, we studied whether the growth inhibition of cancer cells was caused by cellular apoptosis.

Table 3. Anti-proliferative activity of **2c** and **3b** against a panel of human cancer cell lines by MTT assay.

To test the induction of apoptosis, A549 cells treated with **3b** and HepG2 cells treated with **2c** for 24 hours were doubly stained with Annexin V/PI (propidium iodide). As shown in figure 2, compounds **3b** and **2c** could effectively induce apoptosis of A549 and HepG2 cells respectively and the effects were dose-dependent. At the 0.5 μM concentration **3b** causes 4.0% late apoptosis annexin V-positive

and PI-positive cells, and the percentage increases to 50.1% at 2.5 μM (Figure 2A). On the other hand, the treatment of HepG2 with **2c** at 10 μM and 20 μM concentrations resulted in 13.9% and 23.7% apoptotic cells respectively (Figure 2B).

Figure 2. A549 cells (A) and HepG2 cells (B) were treated with **3b** and **2c** respectively at the indicated concentrations for 24 hours and analyzed by annexin V/PI staining. The cells undergoing apoptosis were defined as two kinds of apoptosis (early apoptosis annexin V-positive cells and late apoptosis annexin V-positive and PI-positive cells).

mRNA synthesis and transcription in cells are regulated by a series of phosphorylation events involving the carboxyl-terminal domain (CTD) of the largest subunit of RNA polymerase II (RNAPII) (19). Three cyclin-dependent kinases (CDK7, CDK8 and CDK9) which are known to phosphorylate the RNAPII CTD during transcription, primarily phosphorylate the RNAPII CTD at Ser5. Furthermore, CDK9 plays a key role in the phosphorylation at Ser2 of RNAPII CTD. Based on our experiments' data, **2c** and **3b** could induce cancer cells apoptosis and effectively inhibit HIV-1 transcription, so we checked cleaved PARP (the mark of apoptosis), phosphorylated Ser2 (p-Ser2) level and the expression level of CDK9 by using western blot analysis. The western blot analysis showed that the p-Ser2 decreased and the cleaved PARP increased slightly when the concentration of **3b** was about $1\times\text{IC}_{50}$ value, but the changes were obvious when the concentration was about $5\times\text{IC}_{50}$ value in A549 cells after 24 hours treatment (Figure 3A). Analogous results were obtained with **2c** in HepG2 cells, with inhibition of the phosphorylation at Ser-2 of RNAPII CTD and induction of cleaved PARP being observed (Figure 3B). However, both the treatment of A549 cells with **3b** and the treatment of HepG2 with **2c** at $1\times\text{IC}_{50}$, $2\times\text{IC}_{50}$ and $5\times\text{IC}_{50}$ concentration for a period of 24 h had little effect on the level of CDK9's expression (Figure 3). These data supported the conclusion that **3b** and **2c** may not affect the expression of CDK9, but could inhibit the phosphorylation at Ser2 of RNAPII CTD and then induce cancer cells apoptosis.

Figure 3. Western blot analysis of A549 cells after **3b** treatment (A) and HepG2 cells after **2c** treatment (B) for 24 hours, α -Tubulin was used as internal control.

Conclusion

Now, significant numbers of anticancer or anti-HIV lead compounds are indole-based small molecules (32,33). In this study, three novel series of 2,5-disubstituted indole derivatives were designed and efficiently synthesized with good yield. Furthermore, all synthesized compounds were assessed for both their anti-proliferative activity against human cancer cells and HIV-1 inhibition activity which was used as a read-out of cellular activity. Interestingly, many compounds showed both anticancer activity and HIV-1 inhibition activity, so they may have dual utility. Among them, compounds **2c** and **3b** possessing good anticancer activity and excellent HIV-1 inhibition activity were further examined in more detail regarding its cellular mode of action. Annexin V/PI staining and cell cycle analysis indicated that compounds **2c** and **3b** successfully inhibited cell cycle progression and displayed good apoptosis in HepG2 cells and A549 cells respectively. The western blot analysis clearly showed the p-Ser2 decreased, the cleaved PARP increased, and the expression level of CDK9 neither decreased nor increased both in the HepG2 cells treated with **2c** and the A549 cells treated with **3b**. These results implied that **3b** and **2c** may induce cancer cells apoptosis through inhibiting the phosphorylation at Ser2 of RNAPII CTD which is essential in mRNA synthesis. However, further studies are required to determine their roles in preventing HIV-1. Additionally, in our lab further detailed structural modifications at 2nd and 5th positions of indole moiety with various group are being underway to get better analogs with improved efficacy.

Acknowledgements

The project was supported by the National Natural Science Foundation of China (No. 81273400 and No. 81302652). This research was also financially supported by Fujian Science and Technology project (Grant No. 2014N5012).

This article is protected by copyright. All rights reserved.

Conflict of Interest

The authors confirm that this article content has no conflict of interests.

References

1. Ding S., Dudley E., Plummer S., Tang J., Newton R. P. and Brenton A. G. (2008) Fingerprint profile of Ginkgo biloba nutritional supplements by LC/ESI-MS/MS. *Phytochemistry*; 69: 1555-1564.
2. Ahuja P. and Siddiqui N. (2014) Anticonvulsant evaluation of clubbed indole-1,2,4-triazine derivatives: A synthetic approach. *Eur J Med Chem*; 80: 509-522.
3. Ma J.Y., Quan Y.C., Jin, H.G., Zhen X.H., Zhang X.W. and Guan L.P. (2016) Practical Synthesis, Antidepressant, and Anticonvulsant Activity of 3-Phenyliminoindolin-2-one Derivatives. *Chem Biol Drug Des*; 87: 342-351.
4. Zhang M.Z., Mulholland N., Beattie D., Irwin D., Gu Y.C., Chen Q., Yang G.F. and Clough J. (2013) Synthesis and antifungal activity of 3-(1,3,4-oxadiazol-5-yl)-indoles and 3-(1,3,4-oxadiazol-5-yl)methyl-indoles. *Eur J Med Chem*; 63: 22-32.
5. Zhang M.Z., Chen Q. and Yang G.F. (2015) A review on recent developments of indole-containing antiviral agents. *Eur J Med Chem*; 89: 421-441.
6. Radwan M.A.A., Ragab E.A., Sabry N.M. and El-Shenawy S.M. (2007) Synthesis and biological evaluation of new 3-substituted indole derivatives as potential anti-inflammatory and analgesic agents. *Bioorgan Med Chem*; 15: 3832-3841.
7. Álvarez R., Puebla P., Díaz J.F., Bento A.C., García-Navas R., de la Iglesia-Vicente J., Mollinedo F., Andreu J.M., Medarde M. and Peláez R. (2013) Endowing Indole-Based Tubulin Inhibitors with an Anchor for Derivatization: Highly Potent 3-Substituted Indolephenstatins and Indoleisocombretastatins. *J Med Chem*; 56: 2813-2827.
8. Perryman A.L., Zhang Q., Soutter H.H., Rosenfeld R., McRee D.E., Olson A.J., Elder J.E. and David Stout C. (2010) Fragment - Based Screen against HIV Protease. *Chem Biol Drug Des*; 75: 257-268.
9. Ma J.Y., Quan Y.C., Jin, H.G., Zhen, X.H., Zhang X.W. and Guan L.P. (2015) Practical Synthesis, Antidepressant, and Anticonvulsant Activity of 3-Phenyliminoindolin-2-one Derivatives. *Chem Biol Drug Des*;
10. Andreani A., Burnelli S., Granaiola M., Leoni A., Locatelli A., Morigi R., Rambaldi M., Varoli L., Landi L., Prata C., Berridge M.V., Grasso C., Fiebig H.H., Kelter G., Burger A.M. and Kunkel M.W. (2008) Antitumor Activity of Bis-indole Derivatives (1). *J Med Chem*; 51: 4563-4570.
11. Nguyen M., Marcellus R.C., Roulston A., Watson M., Serfass L., Madiraju S.R.M., Goulet D.,

- Viallet J., Belec L., Billot X., Acoca S., Purisima E., Wiegman A., Cluse L., Johnstone R.W., Beauparlant P. and Shore G. C. (2007) Small molecule obatoclax (GX15-070) antagonizes MCL-1 and overcomes MCL-1-mediated resistance to apoptosis. *Proc. Natl. Acad. Sci. U. S. A.*; 104: 19512-19517.
12. Sun L., Liang C., Shirazian S., Zhou Y., Miller T., Cui J., Fukuda J.Y., Chu J.Y., Nematalla A., Wang X., Chen H., Sistla A., Luu T. C., Tang F., Wei J. and Tang C. (2003) Discovery of 5-[5-Fluoro-2-oxo-1,2-dihydroindol-(3Z)-ylidenemethyl]-2,4-dimethyl-1H-pyrrole-3-carboxylic Acid (2-Diethylaminoethyl)amide, a Novel Tyrosine Kinase Inhibitor Targeting Vascular Endothelial and Platelet-Derived Growth Factor Receptor Tyrosine Kinase. *J Med Chem*; 46: 1116-1119.
13. Wu S., Wang L., Guo W., Liu X., Liu J., Wei X. and Fang B. (2011) Analogues and Derivatives of Oncrasin-1, a Novel Inhibitor of the C-Terminal Domain of RNA Polymerase II and Their Antitumor Activities. *J Med Chem*; 54: 2668-2679.
14. Bacher G., Nickel B., Emig P., Vanhoefer U., Seeber S., Shandra A., Klenner T. and Beckers T. (2001) D-24851, a novel synthetic microtubule inhibitor, exerts curative antitumoral activity in vivo, shows efficacy toward multidrug-resistant tumor cells, and lacks neurotoxicity. *Cancer Res*; 61: 392-399.
15. Alexandre F.O.R., Amador A.S., Bot S.P., Caillet C., Convard T., Jakubik J., Musiu C., Poddesu B., Vargiu L. and Liuzzi M. (2010) Synthesis and biological evaluation of aryl-phospho-indole as novel HIV-1 non-nucleoside reverse transcriptase inhibitors. *J Med Chem*; 54: 392-395.
16. Han X., Ouyang W., Liu B., Wang W., Tien P., Wu S. and Zhou H.B. (2013) Enantioselective inhibition of reverse transcriptase (RT) of HIV-1 by non-racemic indole-based trifluoropropanoates developed by asymmetric catalysis using recyclable organocatalysts. *Organic & biomolecular chemistry*; 11: 8463-8475.
17. Ou M. and Sandri-Goldin R.M. (2013) Inhibition of cdk9 during herpes simplex virus 1 infection impedes viral transcription. *PLoS One*; 8: e79007.
18. Ou M. and Sandri-Goldin R. M. (2013) Inhibition of cdk9 during Herpes Simplex Virus 1 Infection Impedes Viral Transcription. *PLoS One*; 8: 16.
19. Kempf C., Bathe F. and Fischer, R. (2013) Evidence that Two Pcl-Like Cyclins Control Cdk9 Activity during Cell Differentiation in *Aspergillus nidulans* Asexual Development. *Eukaryot. Cell*; 12: 23-36.
20. Lam L.T., Pickeral O.K., Peng A.C., Rosenwald A., Hurt E.M., Giltane J.M., Averett L.M., Zhao H., Davis R. E. and Sathymoorthy M. (2001) Genomic-scale measurement of mRNA turnover and the mechanisms of action of the anti-cancer drug flavopiridol. *Genome Biol*; 2: 1-11.
21. Mitri Z., Karakas C., Wei C.M., Briones B., Simmons H., Ibrahim N., Alvarez R., Murray J.L., Keyomarsi K., and Moulder S. (2015) A phase 1 study with dose expansion of the CDK inhibitor dinaciclib (SCH 727965) in combination with epirubicin in patients with metastatic triple negative breast cancer. *Invest New Drug*; 33: 890-894.
22. Mahadevan D., Plummer R., Squires M.S., Rensvold D., Kurtin S., Pretzinger C., Dragovich T., Adams J., Lock V., Smith D.M., Von Hoff D. and Calvert H. (2011) A phase I pharmacokinetic

- and pharmacodynamic study of AT7519, a cyclin-dependent kinase inhibitor in patients with refractory solid tumors. *Annals of oncology: official journal of the European Society for Medical Oncology / ESMO*; 22: 2137-2143.
23. Chen R., Wierda W.G., Chubb S., Hawtin R.E., Fox J.A., Keating M.J., Gandhi V. and Plunkett W. (2009) Mechanism of action of SNS-032, a novel cyclin-dependent kinase inhibitor, in chronic lymphocytic leukemia. *Blood*; 113: 4637-4645.
24. Pumfery A., de la Fuente C., Berro R., Nekhai S., Kashanchi F., and Chao S.H. (2006) Potential use of pharmacological cyclin-dependent kinase inhibitors as anti-HIV therapeutics. *Curr Pharm Design*; 12: 1949-1961.
25. Sancineto L., Iraci N., Massari S., Attanasio V., Corazza G., Barreca M.L., Sabatini S., Manfroni G., Avanzi N. R., Cecchetti V., Pannecouque C., Marcello A. and Tabarrini O. (2013) Computer-Aided Design, Synthesis and Validation of 2-Phenylquinazolinone Fragments as CDK9 Inhibitors with Anti-HIV-1 Tat-Mediated Transcription Activity. *Chemmedchem*; 8: 1941-1953.
26. Houlihan W.J., Parrino V.A. and Uike Y. (1981) Lithiation of N-(2-alkylphenyl)alkanamides and related compounds. A modified Madelung indole synthesis. *The Journal of Organic Chemistry*; 46: 4511-4515.
27. Robinson M.W., Overmeyer J.H., Young A.M., Erhardt P.W. and Maltese W.A. (2012) Synthesis and Evaluation of Indole-Based Chalcones as Inducers of Methuosis, a Novel Type of Nonapoptotic Cell Death. *J Med Chem*; 55: 1940-1956.
28. Li L., Zhao H., Wang J. and Wang R. (2014) Facile Fabrication of Ultrafine Palladium Nanoparticles with Size- and Location-Control in Click-Based Porous Organic Polymers. *ACS Nano*; 8: 5352-5364.
29. Yang L.L., Li G.B., Ma S., Zou C., Zhou S., Sun Q.Z., Cheng C., Chen X., Wang L.J. and Feng S. (2013) Structure–activity relationship studies of pyrazolo [3, 4-d] pyrimidine derivatives leading to the discovery of a novel multikinase inhibitor that potently inhibits FLT3 and VEGFR2 and evaluation of its activity against acute myeloid leukemia in vitro and in vivo. *J Med Chem*; 56: 1641-1655.
30. Patel S.R., Gangwal R., Sangamwar A.T. and Jain R. (2015) Synthesis, biological evaluation and 3D QSAR study of 2,4-disubstituted quinolines as anti-tuberculosis agents. *Eur J Med Chem*; 93: 511-522.
31. Yik J.H.N., Chen R.C., Nishimura R., Jennings J.L., Link A.J. and Zhou Q. (2003) Inhibition of P-TEFb (CDK9/Cyclin T) kinase and RNA polymerase II transcription by the coordinated actions of HEXIM1 and 7SK snRNA. *Mol Cell*; 12: 971-982.
32. Ma J.J., Bao G.L., Wang L.M., Li W.T., Xu B.X., Du B.G., Lv J., Zhai X. and Gong P. (2015) Design, synthesis, biological evaluation and preliminary mechanism study of novel benzothiazole derivatives bearing indole-based moiety as potent antitumor agents. *European Journal of Medicinal Chemistry*; 96: 173-186.
33. Ashok P., Lu L.C., Chander S., Zheng Y.T. and Murugesan S. (2015) Design, Synthesis, and Biological Evaluation of 1-(thiophen-2-yl)-9H-pyrido[3,4-b]indole Derivatives as Anti-HIV-1

Supporting Information

Additional Supporting Information may be found in the online version of this article:

Spectra data of compounds **1b~1e**, **2a~2b**, **2d~2p**, **3a** and **3c~3s**.

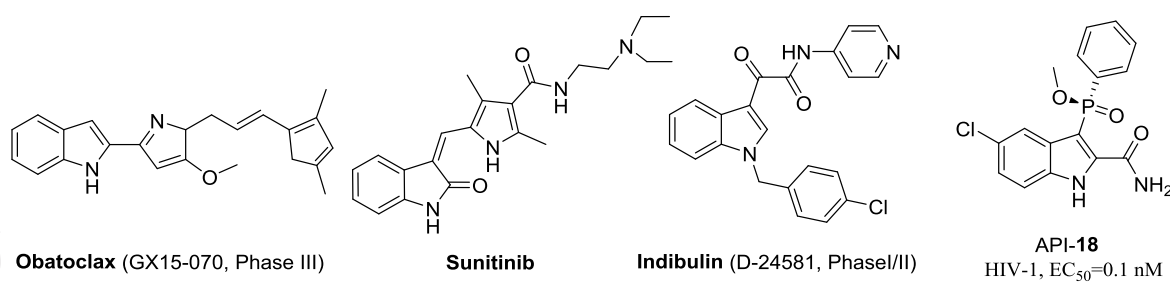


Figure 1. Structures of four compounds bearing indole-based moiety

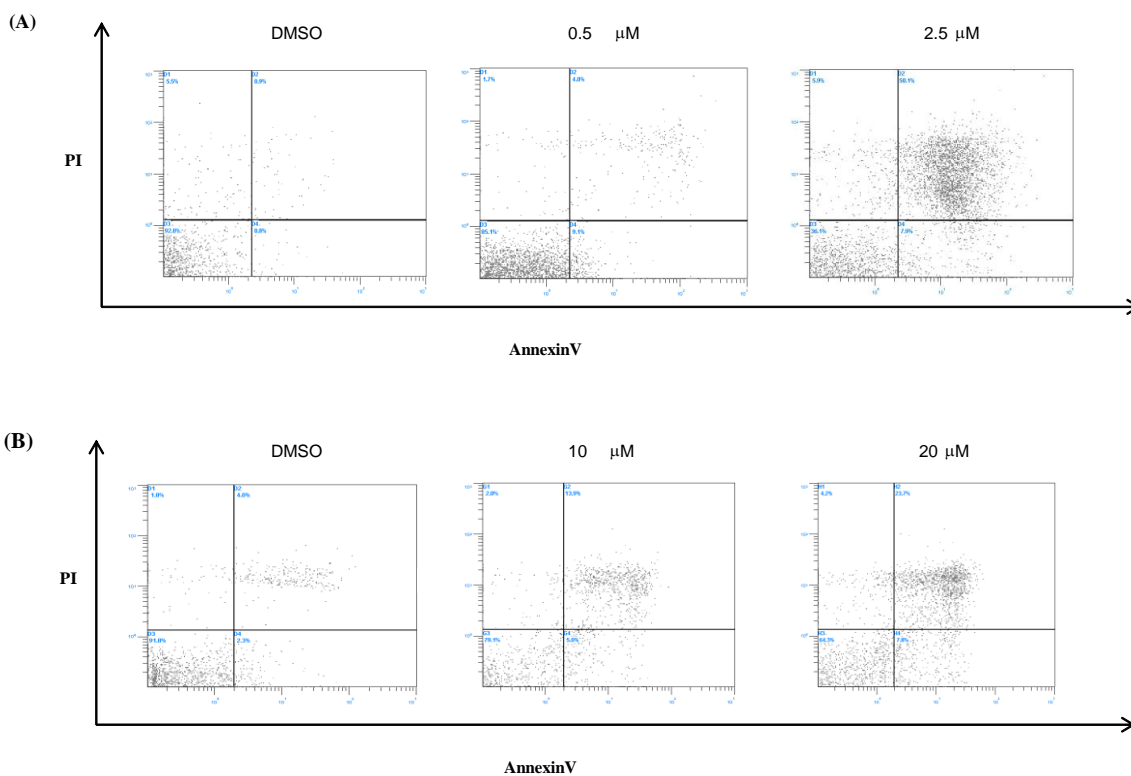


Figure 2. A549 cells (A) and HepG2 (B) cells were treated with **3b** and **2c** respectively at the indicated concentrations for 24 hours and analyzed by annexin V/PI staining. The cells undergoing apoptosis were defined as two kinds of apoptosis (early apoptosis annexin V-positive cells and late apoptosis annexin V-positive and PI-positive cells).

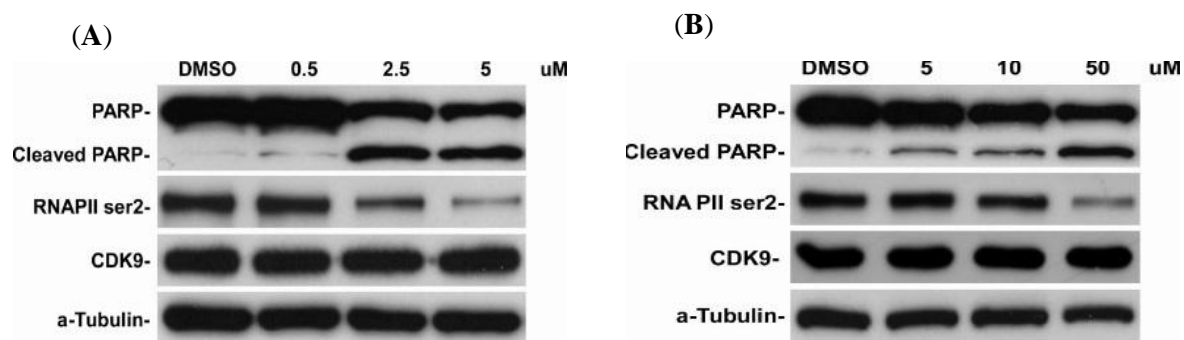
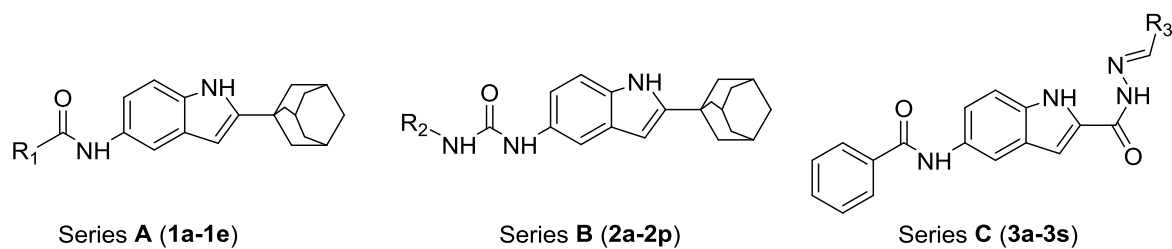
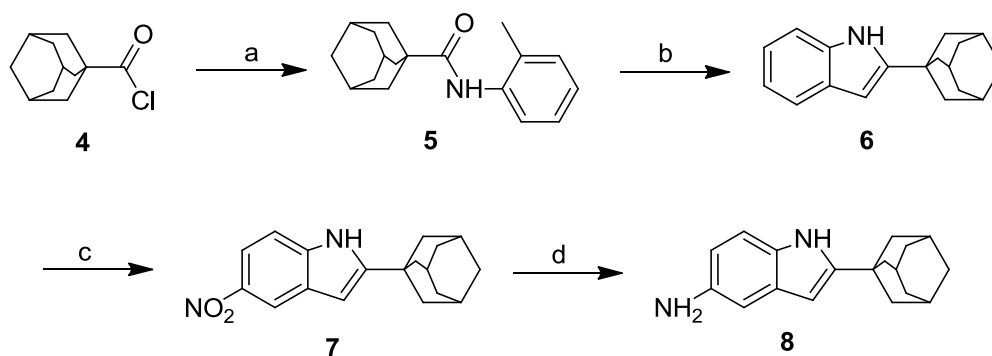


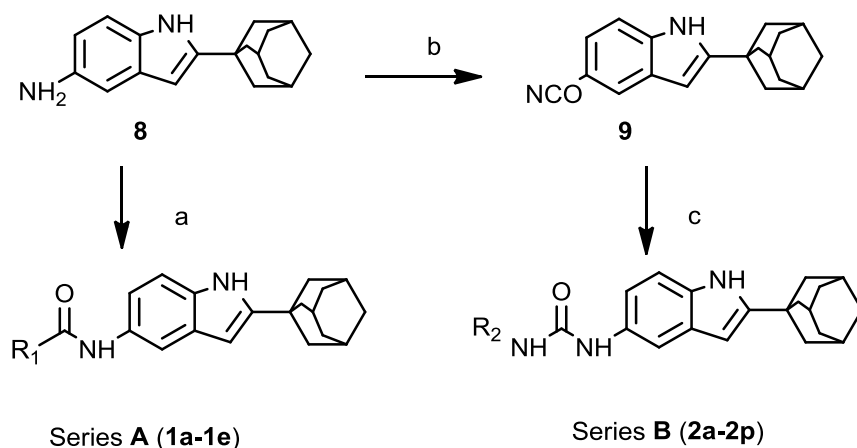
Figure 3. Western blot analysis of A549 cells after **3b** treatment (A) and HepG2 cells after **2c** treatment (B) for 24 hours, a-Tubulin was used as internal control.



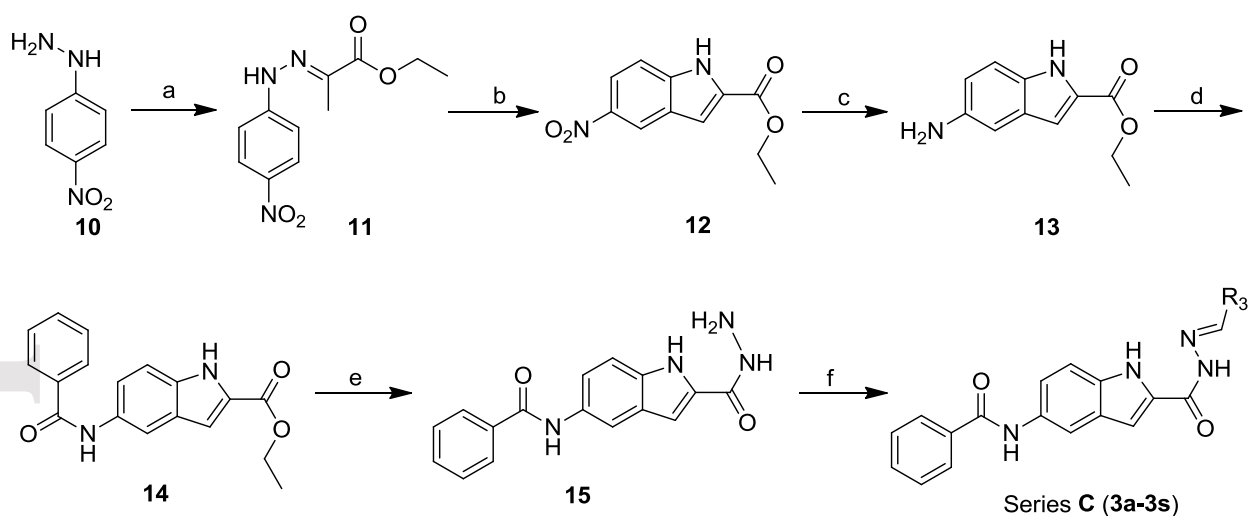
Scheme 1. 2,5-Disubstituted indole derivatives



Scheme 2. Synthesis of 2-(adamantan-1-yl)-1H-indol-5-amine. Reagents and conditions: (a) toluene, *o*-toluidine, K_2CO_3 , r.t., 4 h; (b) *n*-BuLi, THF, $0^\circ C$, N_2 , 3 h; (c) NH_4NO_3 , H_2SO_4 , $0^\circ C$, 1 h; (d) Fe, AcOH, H_2O , EtOH, $70^\circ C$, 2 h.

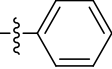
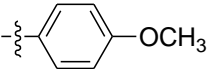
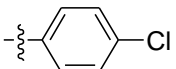
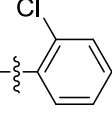
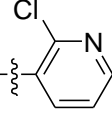
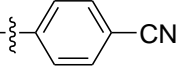
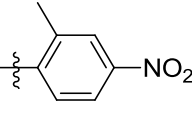
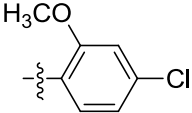
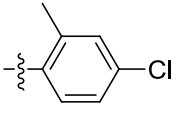
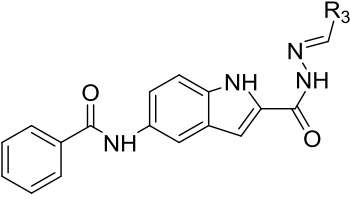


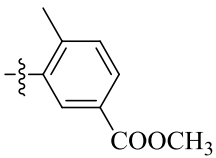
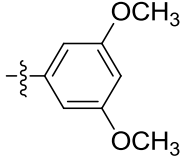
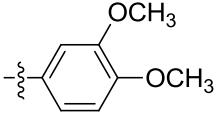
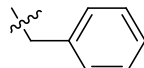
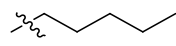
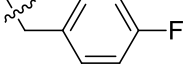
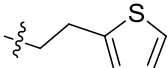
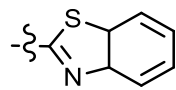
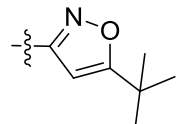
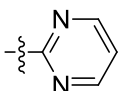
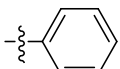
Scheme 3. Synthesis of series A and series B. Reagents and conditions: (a) benzoyl chloride, toluene, 60°C, 8 h; (b) triphosgene, THF, trimethylamine, 0°C, 4 h; (c) R-NH₂, toluene, 60°C, 4 h.

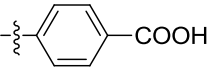
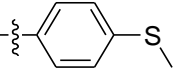
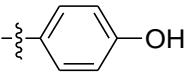
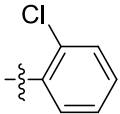
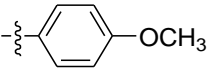
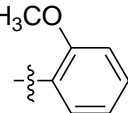
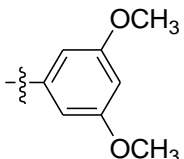
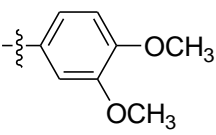
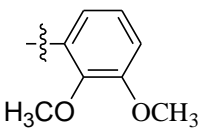
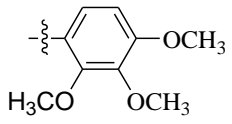
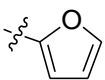
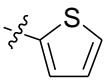


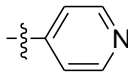
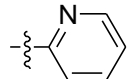
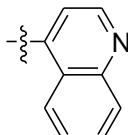
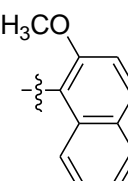
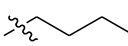
Scheme 4. Synthesis of series C. Reagents and conditions: (a) ethyl 2-oxopropanoate, EtOH, reflux, 2 h; (b) polyphosphoric acid, 100°C, 1 h; (c) Fe, AcOH, H₂O, EtOH, 70°C, 2 h. (d) benzoyl chloride, toluene, 60°C, 8 h; (e) Hydrazine hydrate, EtOH, reflux, 6 h; (f) RCHO, EtOH, reflux, 8 h.

Table 1. Anti-proliferative activity (IC_{50} , μM) against cancer cells of 2,5-disubstituted indole derivatives

Compound	$R_1/R_2/R_3$	IC_{50} (μM) \pm S.D.		
		Hela	HepG2	A549
1a		2.59 \pm 0.08	10.89 \pm 0.12	21.54 \pm 0.05
1b		6.96 \pm 0.10	10.55 \pm 0.05	15.92 \pm 0.12
1c		2.40 \pm 0.05	9.32 \pm 0.07	20.62 \pm 0.11
1d		1.34 \pm 0.08	11.16 \pm 0.09	8.34 \pm 0.10
1e		3.33 \pm 0.11	22.23 \pm 0.12	27.12 \pm 0.13
2a		1.44 \pm 0.05	0.99 \pm 0.08	0.50 \pm 0.06
2b		2.21 \pm 0.09	3.90 \pm 0.06	18.02 \pm 0.10
2c		15.54\pm0.12	13.21\pm0.11	15.92\pm0.09
2d		1.54 \pm 0.05	0.80 \pm 0.04	3.87 \pm 0.09
3a-3s				

2e		34.16±0.11	nd	nd
2f		27.80±0.13	nd	nd
2g		26.30±0.11	nd	nd
2h		31.27±0.11	nd	nd
2i		>100	nd	nd
2j		>100	nd	nd
2k		33.21±0.15	nd	nd
2l		82.56±0.10	nd	nd
2m		>100	nd	nd
2n		2.77±0.08	3.64±0.09	6.41±0.10
2o		12.58±0.12	3.65±0.05	3.04±0.08
2p		9.42±0.10	6.93±0.09	13.92±0.12
3a		>100	nd	nd

3b		8.70±0.11	2.93±0.09	0.48±0.05
3c		10.88±0.15	9.08±0.10	2.58±0.09
3d		7.30±0.13	1.41±0.08	0.16±0.05
3e		46.06±0.13	nd	nd
3f		58.30±0.14	nd	nd
3g		>100	nd	nd
3h		>100	nd	nd
3i		1.67±0.07	3.22±0.05	1.41±0.05
3j		>100	nd	nd
3k		>100	nd	nd
3l		22.16±0.13	nd	nd
3m		18.91±0.11	24.08±0.16	12.08±0.17
3n		>100	nd	nd

3o		>100	nd	nd
3p		18.41±0.15	11.24±0.10	6.26±0.09
3q		24.70±0.08	nd	nd
3r		73.50±0.20	nd	nd
3s		>100	nd	nd
DDP		4.52±0.10	6.10±0.09	1.83±0.05

Each compound was tested in sextuplicate, nd: not determined. The error bars in all panels represent mean ± SD from three independent experiments.

Table 2. HIV-1 inhibition activity

Compound	Concentration (μM)			Compound	Concentration (μM)		
	0.2	2.0	20		0.2	2.0	20
1a	0.84±0.02	0.74±0.05	0.70±0.02	2a	1.10±0.10	0.67±0.06	0.44±0.02
2b	1.00±0.09	0.91±0.08	0.45±0.05	2c	0.86±0.02	0.56±0.02	0.29±0.01
2d	0.86±0.03	0.86±0.05	0.67±0.03	2e	1.01±0.10	1.00±0.09	0.30±0.04
2f	1.00±0.09	0.84±0.07	0.32±0.04	2h	1.04±0.10	0.77±0.07	0.11±0.03

2k	0.95±0.08	0.90±0.07	0.28±0.04	2n	0.90±0.09	0.88±0.05	0.59±0.04
2r	0.94±0.10	0.92±0.08	0.18±0.03	2s	1.05±0.08	1.02±0.10	0.15±0.03
2t	1.05±0.11	1.04±0.11	0.25±0.02	3b	0.76±0.06	0.64±0.05	0.26±0.03
3f	0.96±0.08	0.55±0.04	0.27±0.03	3i	0.97±0.09	0.59±0.04	0.43±0.03
3l	0.96±0.10	0.64±0.05	0.33±0.02	3n	0.89±0.09	0.72±0.04	0.47±0.03
3p	1.04±0.09	1.01±0.11	0.35±0.02	3q	1.00±0.09	0.46±0.03	0.23±0.03

Each compound was tested in triplicate. The error bars in all panels represent mean ± SD from three independent experiments.

Table 3. Anti-proliferative activity of **2c** and **3b** against a panel of human cancer cell lines by MTT assay.

Compound	Human cell line 48h –MTT IC ₅₀ (μM) ± S.D.				
	HeLa	MCF-7	HePG2	H460	A549
2c	15.54±0.08	19.30±0.35	13.21±0.30	31.92±0.35	15.92±0.25
3b	8.70±0.06	5.10±0.11	2.93±0.45	1.90±0.55	0.48±0.15

Each compound was tested in sextuplicate. The error bars in all panels represent mean ± SD from three independent experiments.